PCCP

Cite this: *Phys. Chem. Chem. Phys.*, 2012, **14**, 8653–8661

www.rsc.org/pccp

PAPER

Electrochromic enhancement of latent fingerprints by poly(3,4-ethylenedioxythiophene)†

Rachel M. Brown and A. Robert Hillman*

Received 7th March 2012, Accepted 2nd May 2012
DOI: 10.1039/c2cp40733g

Spatially selective electrodeposition of poly-3,4-ethylenedioxythiophene (PEDOT) thin films on metallic surfaces is shown to be an effective means of visualizing latent fingerprints. The technique exploits the fingerprint deposit as an insulating mask, such that electrochemical processes (here, polymer deposition) may only take place on deposit-free areas of the surface between the ridges of the fingerprint deposit; the end result is a negative image of the fingermark. Use of a surfactant (sodium dodecylsulphate, SDS) to solubilise the EDOT monomer allows the use of an aqueous electrolyte. Electrochemical (coulometric) data provide a total assay of deposited material, yielding spatially averaged film thicknesses, which are commensurate with substantive filling of the trenches between fingerprint deposit ridges, but not overfilling to the extent that the ridge detail is covered. This is confirmed by optical microscopy and AFM images, which show continuous polymer deposition within the trenches and good definition at the ridge edges. Stainless steel substrates treated in this manner and transferred to background electrolyte (aqueous sulphuric acid) showed enhanced fingerprints when the contrast between the polymer background and fingerprint deposit was optimised using the electrochromic properties of the PEDOT films. The facility of the method to reveal fingerprints of various ages and subjected to plausible environmental histories was demonstrated. Comparison of this enhancement methodology with commonly used fingerprint enhancement methods (dusting with powder, application of wet powder suspensions and cyanoacrylate fuming) showed promising performance in selected scenarios of practical interest.

Introduction

Fingerprints have been used as a means of biometric identification since the mid 1800s and, despite the rise of other methods such as those based on DNA, remain a cornerstone of the identification of individuals for forensic and other purposes. Accordingly, the last century has seen great innovation of physical and chemical methods for visualizing fingerprints on diverse surfaces.[1] Nevertheless, the reality is that the success rate in extracting fingerprints of adequate quality for unequivocal identification remains low – in the case of metallic surfaces, only a few percent.[2–4] While incremental improvements to existing methods undoubtedly have value, it is clear that substantive progress requires the advent of radically different approaches. Here we describe one such approach, the basis of which requires an order of magnitude less fingerprint residue than typical methods and the nature of which introduces the additional dimension of externally variable optical properties to optimise visual contrast.

Department of Chemistry, University of Leicester, Leicester, LE1 7RH, UK. E-mail: arh7@le.ac.uk
† Electronic supplementary information (ESI) available. See DOI: 10.1039/c2cp40733g

The attractions of using fingerprints for identification are that they are unique to an individual,[1] are unchanged throughout life, can survive superficial damage to the skin[1] and persist for a significant time after death.[5] Their intricate spatial form also means that it is extremely difficult to "contaminate" an object with a perfectly formed fingerprint. Formation of a fingermark on a surface is an example of the classic Locard's principle,[6,7] commonly expressed as "*every contact leaves a trace*". There are three types of fingermark: *patent* (in which the transfer of a coloured substance leaves a visible image), *plastic* (when pressure from the finger on a soft material leaves a 3D imprint) and *latent* (when the material exchanged with the surface is not visible).[1] The last of these is the most common source of forensic evidence but, by definition, such fingerprints require treatment to reveal the image.

Most latent fingerprints are attributable to secretions from two types of sweat gland: eccrine glands found on the hands and sebaceous glands found on the facial areas. Eccrine sweat has a very high water content,[1] in which the predominant solutes are inorganic salts (some at a sufficiently high concentration to corrode metal surfaces[8]) as well as lipids and amino acids, whose presence is exploited in fingerprint development with ninhydrin. Sebaceous sweat comprises a complex mixture of fatty acids,

phospholipids, wax esters, sterols and squalene, collectively referred to as *sebum*.[1]

Broadly speaking, current fingerprint development methods involve interaction of the chosen reagent with one of the water soluble or lipid components of the sweat deposit; lack of knowledge of the fingerprint history introduces uncertainty into the enhancement process. Traditional reagents and delivery methods include dusting with powders (of a fluorescent,[9–11] magnetic[1,12,13] or thermoplastic nature), dipping in (or spraying with) ninhydrin solution,[14] vacuum metal deposition,[15] small particle reagent,[15] physical developer[15] and fuming with cyanoacrylate[16,17] ("superglue"). In the latter instance, the white polymeric product is commonly visualized by soaking in solutions of basic dyes such as Basic Yellow 40, Rhodamine 6G (Basic Red 1), Safranine O (Basic Red 2) and Basic Red 14 and the objects viewed under fluorescent conditions. A variant of the fluorescence approach is the use of cadmium sulphide nanocomposites, which bond with the fatty acid and amino acid components in fingerprint deposits.[18] Recent physically-based approaches include using a Scanning Kelvin Probe[19,20] to map surface work function variations and high voltage-driven spatially selective local adhesion of carbon particulates to semi-conducting oxides formed on brass surfaces (*e.g.* bullet casings).[21]

While analysis of the complex spatial patterns of fingerprints[22] is not the focus of the present work, an appreciation of their form is required to define the challenge of their visual enhancement. Fingerprint detail is considered at three levels. First level detail describes the general type of fingerprint pattern: a loop, a whorl or an arch. Second level detail corresponds to characteristic *minutiae* within the fingerprint: a *ridge ending*, a *bifurcation*, a *lake* (where two split ridges rejoin after a bifurcation), a *dot*, an *island* (a short independent ridge), a *spur* or a *crossover* (running between two parallel ridges). Third level detail corresponds to smaller features, such as pores, on the ridges. First level detail clearly cannot provide identification, but can be useful for elimination purposes.[1] Currently, the spatial relationship between – though not the identity of – second level features is the basis of fingerprint identification; their unambiguous imaging is thus critical. Third level detail, which is commonly not resolved, is not presently used in isolation for identification purposes. However, it may be used in combination with second (or even first) level detail in a holistic approach, exploiting all the available information to reach a decision on identification. Thus, techniques capable of resolving third level detail hold considerable future promise, notably for partial fingerprints or other situations where unambiguous second level detail is sparse.

We now report the successful implementation of a new concept, based on the use of the fingerprint deposit as a template, or "mask", through which the visualizing reagent may be deposited, to give a negative image of the fingerprint. The approach is complementary to most visualization methods, in that it involves interaction *not* with the fingerprint but with the *uncovered* regions of the substrate. This first stage of the concept (illustrated in Scheme 1) was described by Bersellini *et al.*,[23] who deposited polypyrrole electrochemically on fingerprinted metal surfaces such as Pt, Au, Ag and Ergal (Al alloy).[23] The fundamental extension pursued here is subsequent potential control of the deposited polymer to vary its optical properties,

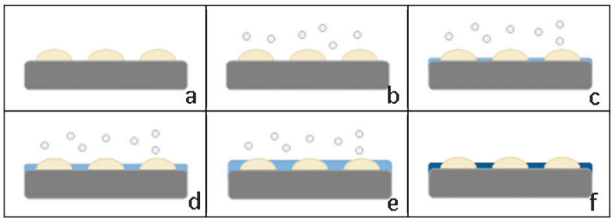

Scheme 1 Schematic representation of strategy for visualizing latent fingerprints by deposition of electrochromic polymer. Panel *a*: surface with deposited fingerprint, prior to treatment; panel *b*: fingerprinted surface immersed in monomer solution, prior to initiation of film deposition; panel *c*: regions of bare (inter-ridge) surface covered with thin layer of polymer in early stages of deposition; panel *d*: surface optimally covered with polymer; panel *e*: excess polymer deposited, resulting in overfilling of trenches and partial obscuring of fingerprint deposit; panel *f*: sample after transfer to monomer-free electrolyte and held at a different potential, generating a contrasting image (*via* a colour change) to that in panel *d*.

i.e. colour. The practical significance of this is that one can then optimise fingerprint visual contrast, yielding excellent second level detail and significant third level detail.

Irrespective of the detailed fingerprint composition (*vide supra*), the premise is that it contains sufficient non-conductive material to form an insulating mask on the surface. Electron transfer – and thus polymer deposition – is prevented by an insulating layer only a few nanometres thick. Since the initial fingerprint deposit may be several microns thick,[24] one only requires retention of a small fraction of the initially deposited material – far less than would be commonly required to give a visible mark by interaction with traditional chemical enhancement agents. The practical significance of this is the potential to image old fingerprints or ones that have been subjected to environmental deterioration.

A preliminary communication demonstrated the electrochromic enhancement concept using polyaniline as the active material.[25] We now implement this strategy using poly(3,4-ethylenedioxythiophene), PEDOT, a widely studied conducting polymer[26–32] with excellent (electro)chemical stability and electrochromic properties. In principle, with a wide operating potential range, one could access three states of distinct optical properties: *n*-doped, undoped and *p*-doped.[33] However, for practical reasons, we elect to operate in aqueous media – facilitated by using a surfactant to effect micellar monomer solubilisation – and thus focus on the interchange of the latter two redox states, which are readily accessible within the aqueous potential window under the conditions employed.

Summarizing the preceding arguments, the generic goal is visualization of latent fingerprints on metallic objects, for the overwhelming majority of which conventional methods do not yield useable images. Specific objectives related to the present study include (i) identification of conditions (media and electrochemical protocols) for PEDOT deposition that do not simultaneously degrade the fingerprint; (ii) demonstration of PEDOT electrochromic enhancement of latent fingerprints; (iii) morphological characterization distinguishing trench filling (desired) from ridge coverage (undesired), showing directly that the PEDOT deposit yields a faithful image of the fingerprint deposit; and (iv) demonstration that enhancement with PEDOT as the active agent is competitive with existing methods. This report

focuses on fundamental aspects of these objectives, extending the polyaniline-based proof-of-concept;[25] complementary performance aspects are the subject of a parallel report.[34] As we shall show, PEDOT deposition from aqueous media provides a powerful means of latent fingerprint enhancement on metals, with access to second and third level detail *via* the added visual dimension of electrochromism.

Experimental

Materials

PEDOT films were deposited from aqueous 0.01 mol dm^{-3} EDOT (Sigma Aldrich)/0.1 mol dm^{-3} H_2SO_4, (Sigma Aldrich), in selected cases (see figure legends) also containing either 0.01 mol dm^{-3} sodium dodecylsulphate (SDS) (Sigma Aldrich) or 0.02 mol dm^{-3} sodium N-lauroylsarcosinate (SLS) (Sigma Aldrich) to facilitate solubilisation of EDOT monomer. All reagents were used as supplied. Subsequent cyclic voltammetric measurements for film characterization and coulometric assay involved exposure of the films to nitrogen-purged aqueous 0.1 mol dm^{-3} H_2SO_4, in selected instances (see figure legends) with SDS or SLS present.

For exploratory purposes, four deposition solution formulations were used: (i) 0.1 mol dm^{-3} $LiClO_4$/0.07 mol dm^{-3} SDS/0.05 mol dm^{-3} EDOT; (ii) 0.1 mol dm^{-3} KCl/0.1 mol dm^{-3} SDS/0.01 mol dm^{-3} EDOT; (iii) 0.1 mol dm^{-3} H_2SO_4/0.01 mol dm^{-3} SDS/0.01 mol dm^{-3} EDOT; (iv) 0.1 mol dm^{-3} H_2SO_4/0.02 mol dm^{-3} SLS/0.01 mol dm^{-3} EDOT. For reasons described below, formulation (iii) was used most extensively.

The substrates were stainless steel 304 plates (2.5 cm × 2.5 cm × 0.08 cm; one face insulated to give an exposed (electrochemically active) geometric area, A = 6.25 cm^2). These were incorporated as the working electrode in a single compartment three-electrode cell, with a Pt flag counter electrode and a Ag/AgCl/KCl (saturated) reference electrode, against which all potentials were controlled and are quoted.

Reagents and associated procedures for standard fingerprint visualization methods (for comparison purposes) are described in the Supporting Information.†

Instrumentation

Electrochemical measurements were made under potential control using a μAUTOLAB type II potentiostat. Optical microscopy images were taken with a Meiji Techno MT7100 trinocular microscope operated by uEye (IDS GmbH). The atomic force microscope (AFM) was a Veeco Dimension 3100 Scanning Probe Microscope operated by a computer using Nanoscope 6.12rl software. The silicon nitride tips were supplied by Veeco (model: RTESP; part: MPP-11100-10). Calibration was effected by scanning over a silicon wafer reference. Images (100 μm × 100 μm) were acquired in tapping mode (resonant frequency 200 kHz) at a scan rate of 0.6 Hz, *i.e.* 120 μm s^{-1}.

Procedures

The metal substrates were washed to remove any protective grease and one side polished with Brasso to a mirror finish. They were then washed again with warm soapy water and acetone to remove the excess polish and left to dry at room temperature. In separate experiments, eccrine and sebaceous fingerprints were analysed. In both cases, donors first washed their hands with soapy water to remove contaminants. Eccrine fingerprints were produced by the donor wearing powder-free nitrile gloves for 2 h, then depositing the print. Sebaceous fingerprints were generated by rubbing the fingertips around the forehead and nose area prior to deposition. In both cases, minimal force was used: this minimizes distortion and provides a more realistic test of any enhancement method. The data presented are representative of fingerprints from a range of donors; the operational implications of their attributes (characteristics such as age and gender) are outside the scope of the present fundamental study.

Potentiodynamic and potentiostatic control functions were explored for EDOT polymerization. Deposition *via* potentiodynamic mode typically involved 20 cycles (guided by visual appraisal of film development) with a cathodic potential limit in the range −0.6 to −0.5 V and an anodic potential limit of 0.9 to 1.2 V at scan rates in the range $20 < v/\text{mV s}^{-1} < 100$. Potentiostatic deposition was in the range 0.9 to 1.2 V for times in the range 140–3600 s. Conditions specific to a given experiment are listed in the relevant figure legend but, in general for the fingerprint application considered here, films produced in the absence of H_2SO_4 were either uneven (beyond the variations imposed by fingerprint deposit) or failed to show electrochromic behaviour. As described below, films deposited under potentiostatic control gave the best outcomes in terms of image contrast; irrespective of the deposition control function, films were transferred to monomer-free electrolyte and characterized potentiodynamically. All measurements were made at room temperature (20 ± 2 °C).

Image interpretation

Coulometric assays of PEDOT surface coverage were made on films immersed in nitrogen-purged, monomer-free 0.1 mol dm^{-3} H_2SO_4. For voltammetric measurements the potential limits were −0.8 V to 0.8 V. Scan rates in the range $1 < v/\text{mV s}^{-1} < 250$ were used to establish complete film electroactivity (or otherwise); for coulometric assay the optimum scan rate for films of sufficient optical density to be practically useful was $v = 30$ mV s^{-1}. The total charge (Q/C) was used to estimate the laterally spatially averaged population density (Γ/mol cm^{-2}) using

$$\Gamma = \frac{Q}{nFA} \qquad (1)$$

where $n = 0.33$ is the maximum doping level during oxidation,[35] F is the Faraday constant and A (/cm^2) is the total exposed electrode area. We note that removal of oxygen, and thereby minimization of the partial current associated with oxygen reduction, is critical to accurate coulometric assay of deposited polymer in a fundamental study but that this would not be required in practical application. In the latter instance, one simply wishes to use applied potential to establish a particular oxidation state (colour); the charge required to do so is not a measured parameter. Since oxygen is not electroactive in the potential range used for EDOT polymerization, its removal at that stage is also not critical.

As discussed in more detail in the supporting information, while eqn (1) provides an unequivocal coulometric assay of the

total amount (moles) of polymer present on the surface, the spatial distribution – both laterally and vertically – requires more careful consideration. If the polymer were deposited as a uniform, dense (unsolvated) slab on the surface, its thickness would be:

$$h^0_{f,av} = \frac{\Gamma}{c} \quad (2)$$

where the zero superscript signifies the absence of solvent, the "av" subscript signifies a laterally averaged value and c is the concentration of monomer units in the film (approximated at the reciprocal of monomer molar volume). The fact that the *lateral* distribution of polymer is *not* uniform is, of course, the entire basis of the methodology presented here. Although there are variations from sample to sample, in a typical situation, the deposited fingermark obscures *ca.* 50% of the surface so, in those unobscured ("bare") regions of the surface where electrochemistry does occur, the local film thickness, $h^0_f \sim 2h^0_{f,av}$. Further, *in situ* solvation of electroactive polymers is known to occur and in this configuration will swell the film *vertically*. Anecdotally, it is accepted that electroactive polymer film solvent volume fractions vary with polymer charge state, solvent and electrolyte composition, but they are commonly in the range 0.2–0.5, *i.e.* may swell the polymer by a further factor of up to two ($1.25\ h^0_f \leq h_f \leq 2\ h^0_f$). To summarize, the total population of polymer is unambiguously known, but local estimates of film thickness require some (reasonable) assumptions.

Images of full PEDOT enhanced fingerprints were captured using a Canon A480 digital camera and digitally enhanced using the GNU Image Manipulation Program 2.6.7 (GIMP). Details of fluorescence, lighting, filters and still image capture for fingerprints enhanced by standard methods are given in the Supporting Information.† In different instances, films were viewed either *ex situ* or under potential control *in situ*; details are given in the figure legends.

Fingerprint images prior to and subsequent to enhancement were graded according to the Bandey scale[36] (see Supporting Information for details†), a five point scale running from 0 (no development) to 4 (full development). Although this scale is designed for research rather than legal application, it is broadly accepted that images of grades 3 and 4 would provide unequivocal (legally undisputed) identification.

Results

Electrochemistry and overview of PEDOT films

PEDOT film quality was judged *visually* by evenness of colour on non-fingerprinted sample regions and by uniformity of ridge definition across the fingerprinted area, *electrochemically* by charge injection/recovery as functions of potential scan rate and repetitive cycling, and *morphologically* by microscopic imaging. Details of these individual assessments are given below, but the summary is that the highest quality films were generated from EDOT deposition solutions containing H_2SO_4 and SDS, and vigorously stirred immediately prior to use to ensure good monomer dispersion. Accordingly, we focus here on PEDOT films deposited potentiostatically (at $E = 0.9$ V) from such solutions; comments on the outcomes for less effective protocols are provided in the Supporting Information.†

These films had electrochemical signatures (voltammetric i–E curves in oxygen-free background electrolyte) typical of relatively thick PEDOT films[32,37] (see Supporting Information†). We do not explore the details of coupled electron/ion (dopant) transfer, which have been discussed previously for diverse electrolytes,[38] save to note the practically critical feature that voltammetric currents were linear with potential scan rate and (necessarily) that injected/recovered charge was independent of scan rate in the range $1 < v/\text{mV s}^{-1} < 250$. These films were stable to extended potential cycling in the range $-0.4 < E/\text{V} < 0.8$; within this range the electrochemical response was attributable solely to PEDOT (no solvent decomposition) and full (un)doping could be accomplished. Although not required for practical purposes, reasonable stability to application of more extreme potentials (from a cathodic limit of $E = -1.4$ V to an anodic limit of $E = 1.5$ V) was found; beyond this range the severe gas evolution associated with solvent decomposition resulted in film rupture. (At least in the case of the cathodic limit, at which the film will be reduced and very resistive, we recognize that ohmic drop may be significant, so the applied potential may not reflect the potential at the film/solution interface.) Films subject only to the potential regime $-0.8 < E/\text{V} < 0.8$ showed electrochromism that could be regenerated by re-immersion in background electrolyte after extended dry storage, were not detached from the surface by washing with water or acetone, but could be damaged by abrasion (*e.g.* scratching the surface).

Based on coulometric assay (see eqn (1) and (2)), the range of film thickness explored was $83 < h^0_{f,av}/\text{nm} < 530$. As discussed above (see Experimental procedures and supporting information), the implication is that local solvated film thickness values were in the range $0.33 < h_f/\mu\text{m} < 2.1$. Quite generally, the height of a fingerprint deposit can range from 10 nm to 2 μm, according to the amount of sweat present on the finger and the pressure applied during deposition,[39] so the selected h_f range spans low level filling (Scheme 1, panel *c*) to overfilling (Scheme 1, panel *e*) of the trenches; this distinction is explored below using AFM imaging. Based on literature data for PEDOT optical properties,[40] the peak absorbances of PEDOT films in this coverage (Γ) range should lie in the ranges 0.4–2.4 and 0.2–1.1 when the films are maintained in the undoped and p-doped states, respectively. Although transmission measurements cannot be made on the metal substrates (and in any case would not be meaningful for films that are, necessarily in this situation, laterally varying in thickness), this estimated absorbance range is consistent with both the needs of visual fingerprint appraisal (*i.e.* giving images whose film/fingerprint deposit contrast gave feature definition at the grade 3 or 4 level on the Bandey scale; see Supporting information†) and the observation that films were readily visible but not totally opaque.

PEDOT electrochromic enhancement – the effect of applied potential

A representative example of latent fingerprint enhancement on a stainless steel substrate is shown in Fig. 1 for the case of a three day old fingerprint stored under ambient conditions. Panel *a* shows the latent sebaceous fingerprint as deposited: while one can deduce qualitatively that there is a fingerprint

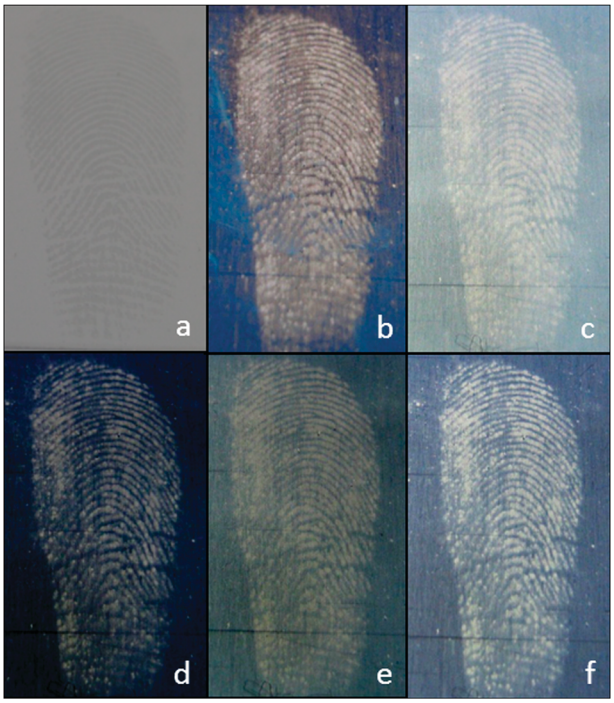

Fig. 1 Effects of ambient medium and applied potential on a fingerprint image subjected to enhancement by PEDOT deposition. All images are for the same sebaceous fingerprint, deposited on stainless steel, then stored for 3 days in ambient laboratory conditions prior to the observations shown. Panel *a*: fingerprint prior to enhancement; panels *b–f* following PEDOT deposition (see main text; deposition time 150 s); final image quality on Bandey scale: grade 3. Sample environment: panel *b*: *ex situ*; panels *c* and *d*: *in situ* exposed to 1 mol dm^{-3} H_2SO_4; panels *e* and *f*: *in situ* exposed to 1 mol dm^{-3} H_2SO_4/0.01 mol dm^{-3} SDS. Applied potential: panels *c* and *e*: 0.80 V; panels *d* and *f*: −0.80 V.

present, there is essentially no ridge detail visible (on the Bandey scale, a grade 0 print). Panels *b–f* show the result of depositing a PEDOT film (from an acidic SDS monomer solution, procedure (iii); see above) and then viewing the enhanced fingerprinted surface under variously controlled conditions. In all cases, it is clear that the image has been significantly enhanced, although differently according to the imposed conditions. For the present, we focus on the effect of applied potential. Comparing panels *c* and *d* and panels *e* and *f* – where each pair corresponds to exposure to the same electrolyte–the result is that active maintenance of the film in a reduced (undoped) state gives a more strongly contrasted image for the case of the stainless steel substrate. In the case of panel *b*, for which the sample was simply removed from the deposition solution, rinsed and viewed *ex situ*, the result is similar to the undoped state. However, while the colour of the PEDOT film is obvious, in this image the full potential (literally) of the method is not realised, since the sample is necessarily not subject to the potential control that allows manipulation of film electrochromic properties between the dark and light blue colours, respectively, of the undoped and p-doped states. For the stainless steel substrate, this is not a significant limitation, but for differently coloured substrates, one might imagine that potential control would be more critical.

Replicate PEDOT deposition experiments on fingerprints of varying ages and subject to different environmental histories (see below) required polymer deposition times on the order of hundreds of seconds (as judged visually to give good contrast). Performance variation with fingerprint age and environmental history has been the subject of a separate operationally-oriented study[34] but transformation of grade 0 images (on the Bandey scale) for an as deposited latent fingerprint to grade 3 or 4 images (as shown in Fig. 1) was commonly achievable for fingerprints left under ambient conditions for extended periods of time. Typically, deposition times in excess of 20 min lead to decreased contrast. The hypothesis, explored below, is that this is a consequence of overfilling the trenches between fingerprint ridges, the scenario represented by panel *e* of Scheme 1.

The *in situ* images of Fig. 1 were acquired with potentiostatic control. More obvious variation of contrast was observed under potentiodynamic conditions, with video recording of the (variably) enhanced image.

Effect of electrolyte composition

Given the widely recognized variation in PEDOT electrochemical (*i–E*) responses in the presence of different electrolytes (a typical feature of conducting polyheterocycle films), the effects of the presence and identity of anionic surfactant were determined. The first of these can be seen by comparison of panels *c* and *e* and panels *d* and *f*. In the latter instance of each pair, the background electrolyte contained SDS; in the former instance of each pair, it did not. Since the two optical responses are different, we deduce that (at least some of) the dodecylsulfonate anion transfers into the film as an anionic dopant upon PEDOT oxidation. If the only dopant were bisulfate (the dominant sulfate species at this pH), then the presence of SDS would make no difference; the fact that it does make a difference unequivocally signals its participation as a transferrable dopant. This differs from the conclusion of Li *et al.*,[41] who deduced that DS^- anions were immobile in Au-supported PEDOT films cycled in SDS and $LiBF_4$. In noting the effect of the presence of SDS in the background electrolyte used for redox cycling the film, it should be recalled that all the images in Fig. 1 relate to the same fingerprint and that those in panels *b–f* all relate to the sample following its PEDOT enhancement from an EDOT/SDS deposition solution. The conclusion here is that the response is predominantly determined *not* by the deposition solution (presence or otherwise of SDS), but rather by the solution to which the film is exposed when the electrochromic effect is exploited.

The fact that anionic surfactant influences film electrochromism prompted the use of a different surfactant, the amino acid-based sodium N-lauroylsarcosinate (SLS), in place of SDS as the solubilising vehicle for EDOT. The outcome, shown in Fig. 2, was a black PEDOT film. Unfortunately, despite the use of apparently similar conditions to a previous report of electrochromism,[42] the fingerprint-templated PEDOT films here did not show an electrochromic response. Practically, the dark film does provide excellent contrast and enhancement for the stainless steel substrate used in Fig. 2, but the loss of electrochromism is in general detrimental.

It was also found that PEDOT films at open circuit showed a response to solution pH. In acidic solution the films were

Fig. 2 Sebaceous fingerprint on stainless steel enhanced by PEDOT deposition from EDOT monomer solution containing 1 mol dm^{-3} H_2SO_4/0.01 mol dm^{-3} SLS. Deposition (3500 s) on freshly fingerprinted surface. Viewed *ex situ*; Bandey scale grade 3.

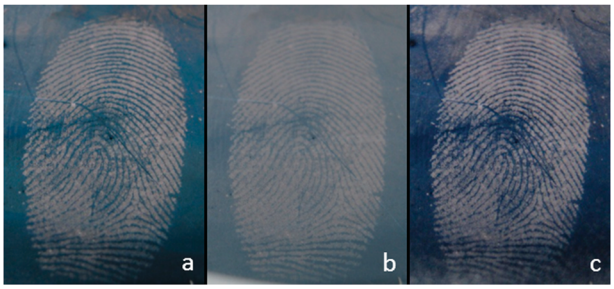

Fig. 3 Effect of pH on PEDOT enhancement for a sebaceous fingerprint on stainless steel (age 24 h under ambient conditions). Panel *a*: *ex situ*; panel *b*: *in situ* immersed in 1 mol dm^{-3} H_2SO_4; panel *c*: *in situ* immersed in 1 mol dm^{-3} KOH (Bandey scale: grade 4).

light blue and in basic solution the films were dark blue colour, as shown in Fig. 3. These are analogous to oxidized and reduced films, respectively, although the basis of this effect is less obvious, given the absence of readily (de-)protonatable sites in PEDOT.

Imaging at different spatial resolution

The visual assessment of fingerprint enhancement was extended by observations at progressively increasing magnification using optical and then atomic force microscopy. Fig. 4 shows a series of optical microscope images of a sebaceous fingerprint kept under water for one day, then enhanced by PEDOT deposition. For illustrative purposes to indicate the spatial resolution of the technique, we show images centred on a representative second level feature (here, a *bifurcation*) that would be used for identification purposes. The contrast between the fingerprint ridge detail and PEDOT deposited between the ridges is excellent. The highest magnification optical image (nominally ×20 magnification; see panel *c*) that contains the entire feature shows its unambiguous and clear outlines. It is clear that, despite the inevitable dissolution of a substantive fraction of the fingerprint deposit, the enhancement procedure is successful.

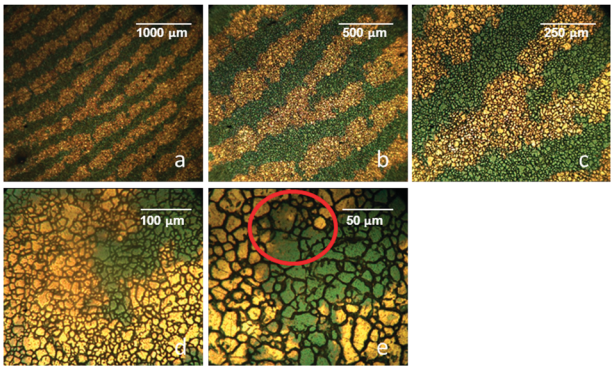

Fig. 4 Optical microscope images (viewed *ex situ*) of progressively increasing magnification (nominally, *a*: ×5; *b*: ×10; *c*: ×20; *d*: ×50; *e*: ×100; see scale bars for absolute dimensions). Fingerprint deposited on stainless steel, kept under water for 1 day, then PEDOT enhanced (see main text; deposition time: 230 s). The images focus in on a second level detail feature, a bifurcation. In panel *e*, red circle highlights onset of overfilling (see main text).

The higher magnification images of Fig. 4 (panels *d* and *e*) are do not contain the full second level feature, but do allow one to inspect the PEDOT/ridge interface. This is relatively sharp, but higher magnification is required to assess this fully. Accordingly, Fig. 5 shows an AFM image of a (necessarily) small section of ridge detail subject to PEDOT enhancement. The fingerprint deposit and PEDOT are morphologically distinct: the PEDOT is rougher and more globular in nature, as seen for many conducting polymer films. The primary issue at stake is the extent of trench (over)filling, as represented in the cartoons of Scheme 1. Specifically, we wish to determine whether the polymer surface population is sufficiently high to be visualized, but sufficiently low that there is still substantial uncovered ridge detail against which the deposited polymer contrasts. In the event that the polymer surface population were too great, the rising level of PEDOT might be expected to spread across the ridge detail (see Scheme 1, panel *e*). While there is some evidence (see red circled area in panel e of Fig. 4) of limited spread of PEDOT across the fingermark ridges, visual appraisal suggests that this does not seem to be widespread. The fundamental reason for this is revealed by images of the type shown in panel *a* of Fig. 5, which shows a slightly surprising – but undoubtedly advantageous – outcome. Although the trench is overfilled, *i.e.* the level of PEDOT is higher than the upper surface of the fingerprint deposit, the PEDOT does *not* flow fully across the ridge. The effect is more obvious in the 1D section across the ridge, shown in panel *b* of Fig. 5, in which the initial fingerprint "ridge" appears as a valley. Practically this is extremely helpful, since one cannot *a priori* know the dimensions of a given fingermark and thus cannot anticipate the optimum polymer coverage, Γ.

Exploring this in more quantitative fashion, the exposed width of the ridge is 26 μm and the PEDOT film rises 300 nm above the top of the fingerprint ridge. Coulometrically, we calculate $h^0_{f,av}$ = 353 nm. In this *ex situ* measurement, it is likely that most of the solvent will have evaporated so, if the film collapses to reflect this fact, then $h^0_f \sim 700$ nm. (If solvent evaporation is not accompanied by film collapse, then the film thickness may be a little larger, but most probably not as large

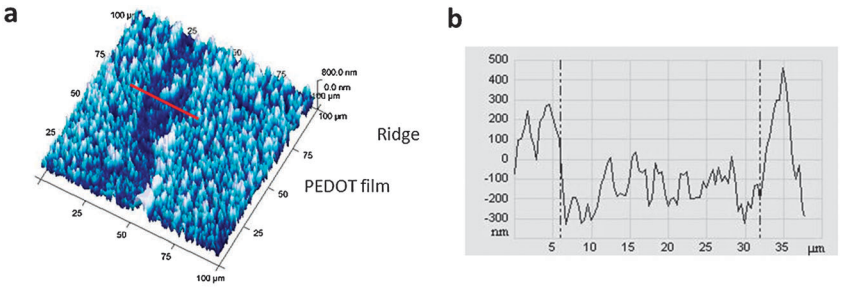

Fig. 5 *Ex situ* AFM image of a section of fingerprint ridge and surrounding PEDOT. Fingerprint was deposited on stainless steel, stored for 11 days under ambient laboratory conditions, then enhanced by PEDOT deposition (250 s). Panel *a*: 3D image; panel *b*: 1D line section perpendicular to ridge (see red line in panel *a*).

as a factor of two for a fully solvated film.) By difference, we deduce that the height of the fingerprint deposit above the metal substrate was 490 nm. According to Thomas *et al.*,[39,43,44] the width of a ridge in a latent fingerprint deposit can be anywhere between 1–50 µm and the height between 10 nm to 2 µm (depending on load when deposited and time elapsed since deposition). The experimental observations fall within these bounds and are consistent with a mid-range deposit that is substantially, but incompletely, covered.

The example of Fig. 5 was a fingerprint aged for 11 days under ambient conditions, during which time evaporation of the more volatile components will have decreased the ridge width and height.[39] From the perspective of a topographic image, this may in part explain the relatively narrow fingerprint ridge and its less regular shape. Loss of volatile components will increase the viscosity of the deposit, making rheological distinction between the viscoelastic[37] PEDOT and fingerprint deposit components less marked. The obvious control experiment of imaging the fingerprint as deposited was not possible due to its fluid-like nature prior to loss of volatile components: the AFM tip was simply dragged through the soft deposit. Nonetheless, the evidence of Fig. 5 is that their different morphological characteristics permit differentiation of the PEDOT and fingerprint deposit components.

Assessment of performance and comparison with existing enhancement techniques

To assess the efficacy of the PEDOT electrochromic enhancement technique, its capability to visualize fingerprints subjected to plausible environmental degradation scenarios was tested. These scenarios were ambient exposure (the least challenging scenario), continuous immersion in water, washing with soap solution followed by ambient exposure, washing with acetone followed by ambient exposure, and continuous exposure to high temperature (150 °C; the most challenging scenario). In each case, samples were imaged after periods of 1, 7, 14 and 28 days. Replicate sets of samples (from different donors) were also treated with three commonly used enhancement methods, namely dusting with black powder, cyanoacrylate ("superglue") fuming followed by dying with the fluorescent yellow dye BY40, and a suspension of iron oxide in detergent (Codeco and distilled water, "Wet Wop"). The empirical outcomes of such a survey executed for five donors are presented elsewhere[34] without explanation of the underlying electrochemistry. Here we focus on these more fundamental issues, through illustrative examples of scenarios where the PEDOT enhancement shows particular promise.

Fig. 6 and 7 show images of PEDOT-enhanced fingerprints previously subjected, respectively, to heat and washing with soap solution. The practical significance of these environments is that both diminish the amount of sweat deposit present on the surface, thereby compromising techniques that involve interaction with the fingerprint itself. For example, traditional techniques (using powder, wet powder and cyanoacrylate ("superglue") treatments) showed poor success rates. Moreover, interest in samples subjected to these environments is motivated by the efficacy of the PEDOT treatment in visualizing these latent fingerprints.[34] For example, across a number of enhancement

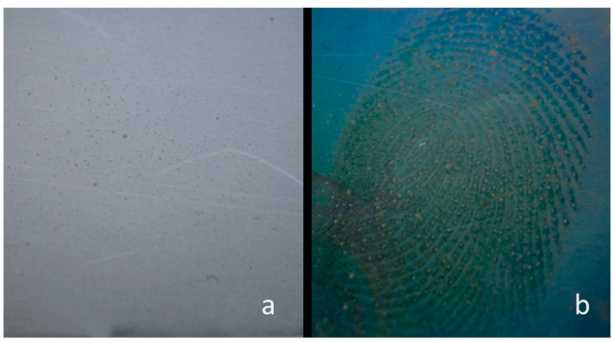

Fig. 6 Images of sebaceous fingerprint kept in an oven at 150 °C for 28 days prior to enhancement with PEDOT. Panel *a*: fingerprint prior to enhancement (Bandey scale: grade 1); panel *b*: *ex situ* after PEDOT deposition (Bandey scale: grade 4).

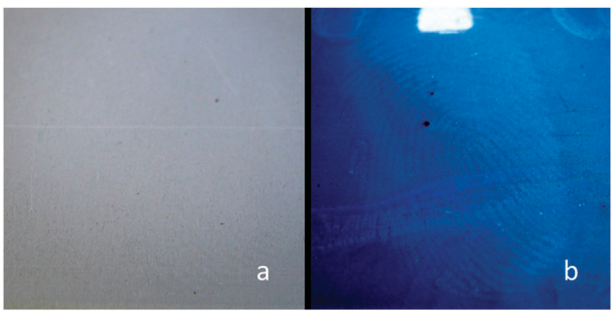

Fig. 7 Images of sebaceous fingerprint hand washed in warm (40 °C) soapy water then kept in ambient conditions for 7 days prior to enhancement with PEDOT. Panel *a*: fingerprint prior to enhancement (Bandey scale: grade 1); panel *b*: *ex situ* after PEDOT deposition (Bandey scale: grade 4).

techniques used to enhance samples subject to heat treatment, PEDOT deposition was responsible over 50% of the successful visualizations, and on 7 day old samples PEDOT showed improved images of 60% of fingerprints washed (with gentle abrasion) with soap solution. For the two examples shown, these high quality PEDOT-enhanced images, showing excellent second level detail and (at least in the case of Fig. 6) significant third level detail, demonstrate clear niche applications for the PEDOT approach.

Although enhancement was possible with both eccrine and sebaceous print residues, sebaceous fingerprints produced higher quality images. We attribute this to the fatty deposits derived from sebaceous fingerprints acting as better insulators and being more resistant to dissolution in the aqueous electrolyte than is the case for the analogous deposits for eccrine fingerprints. Practically, this is beneficial since fingerprints in a forensic context commonly contain a mixture of eccrine and sebaceous sweat. In particular, one rarely finds pure eccrine fingerprint deposits, since they are frequently contaminated with sebaceous residues as a result of contact of the fingertips with the face or hair.

The overall picture, set in the context of complementary and competing methods, is summarised in Fig. 8. This figures aggregates the outcomes of a survey involving over 500 samples, involving fingerprints from different donors, subjected to different environments/histories, sampled after different time intervals and enhanced using different methods. The detailed effects of these parameters from an operational perspective are described elsewhere[34] for the majority of this data set. The purpose of showing the integrated data set is to assert the potential efficacy

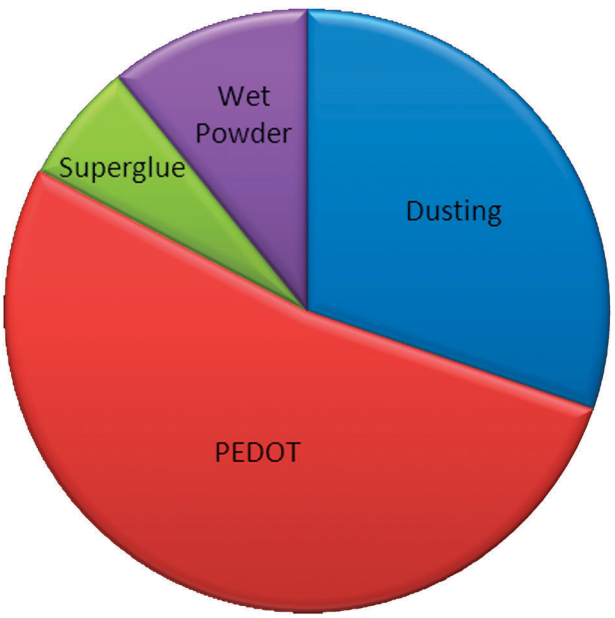

Fig. 8 Summary of success rates (image enhanced to Bandey scale grade 3 or 4) using various latent fingerprint enhancement methods: black powder, wet powder, cyanoacrylate fuming and PEDOT electrochromic polymer (as annotated). For the three traditional methods, survey size was 100 samples each and for PEDOT the survey size was 130 samples. In all cases, samples spanned a range of ages (1–28 days) and environmental exposures (see ref. 34 for details). For each enhancement methodology, the success rate was normalized to the number of samples.

of the electrochromic treatment. The simplistic view is that the PEDOT enhancement method and powder dusting are the two most effective methods, although this superficial assessment conceals the fact that the strengths of the two best methods are somewhat complementary. The poor performance of "superglue" is perhaps surprising, but it should be emphasised that it is an excellent method for imaging latent fingerprints on plastics and other insulating surfaces, for which the electrochromic approach cannot be used.

We end the discussion with some comments on issues related to practitioner uptake of this novel approach. The choice of instrumentation will depend upon the object to be processed, but capital costs need not be more than for the cyanoacrylate (superglue fuming) cabinet that is a feature of every well-founded fingerprint laboratory. There is a wide selection of such instruments commercially available and choice would be based on the current requirement: objects of larger area will require passage of larger current, *i.e.* a potentiostat of greater compliance. Reagent costs are modest. Operation is simple and processing time will be comparable to that of existing chemical treatment techniques. We do not envisage substantial barriers to exploitation associated with typical laboratory infrastructure, safety issues or economic factors.

Conclusions

The principle of using the broadly insulating characteristics of a fingerprint deposit on a metal surface as a mask, or template, for the spatially selective electrodeposition of PEDOT films has been demonstrated. The facility to alter the optical properties – simplistically, colour – of the deposited film *via* the application of an external voltage provides a means to optimise contrast within the image. This introduces a new dimension to fingerprint imaging. Further, the reversibility of this latter process means that one can independently optimise contrast in different regions of the image, for example where the fingerprint deposit is of variable thickness or definition.

For the situations explored – on stainless steel as a representative surface – potentiostatic polymerization of EDOT monomer in an aqueous SDS surfactant dispersion was found to be optimum. Suitable control of deposition rate, *via* monomer concentration and deposition potential and time, permits progressive filling of trenches between fingerprint deposits until optimum contrast is achieved. Both eccrine and sebaceous latent fingerprint deposits were developed on stainless steel, although sebaceous prints provided the highest quality images. This is attributed to the greater insulating nature of the predominantly hydrocarbon-based deposits resulting from these fingerprints.

Microscopic observation of the polymer/fingerprint deposit structures on the surface show good definition. For the particular material used, PEDOT, it turns out that some element of overfilling of the trenches can be tolerated, since the polymer grows preferentially vertically (outwards) rather than laterally (across the top of the fingerprint deposit). While one would naturally attempt to avoid overfilling of the trenches, this may in practice be difficult for marks of variable deposit thickness, so this tolerance has practical value. An additional attractive practical attribute of this system is the option of using

an aqueous electrolyte for both deposition and film redox state variation. In the deposition step, this requires use of a surfactant to solubilise the monomer: limited exploration of surfactant options suggests this may be an additional area for useful optimisation and/or colour manipulation.

From an operational perspective, this method reveals latent fingerprints of evidentially useful quality from challenging and practically relevant situations, including attempts to remove the fingerprint and extended exposure to water or heat. In the latter two instances, it is surmised that this is a result of removal of water-soluble (conducting) components, such that the insulating organic components are concentrated on the surface to provide a more effective template for polymer deposition. In the case of heat treatment, water will also be removed. Across a range of fingerprint histories and ages, PEDOT enhancement outperforms cyanoacrylate and wet powder enhancements. Overall, it has a similar success rate to dusting with black powder, but the strengths of these two reagents are complementary.

The approach of a visualizing reagent interacting with the bare surface is complementary to the majority of fingerprint enhancement methods, which are based on interaction of some reagent with the fingerprint deposit itself. This offers the promise, to be explored in future work, of using both approaches without mutual exclusion. Other areas of future enquiry will include application to other metals, variation of deposition solution formulation (for example using other surfactants with potential generation of different optical properties), and assessment of the extent of third level detail present.

Acknowledgements

We thank Dr John Bond, Dr Karl Ryder and Mark Rowe (Northamptonshire Police) for helpful conversations on practical issues. RMB thanks the University of Leicester for a scholarship.

References

1 H. C. Lee and R. E. Gaensslen, *Advances in Fingerprint Technology*, CRC Press, Boca Raton, 2nd edn, 2001.
2 S. P. Wargacki, L. A. Lewis and M. D. Dadmun, *J. Forensic Sci.*, 2008, **53**, 1138–1144.
3 P. Cuce, G. Polimeni, A. P. Lazzaro and G. De Fulvio, *Forensic Sci. Int.*, 2004, **146**, 7–8.
4 M. Zhang and H. H. Girault, *Analyst*, 2009, **134**, 25–30.
5 R. Fields and D. K. Molina, *J. Forensic Sci.*, 2008, **53**, 952–955.
6 A. R. W. Jackson and J. M. Jackson, *Forensic Science*, Pearson Prentice House, Harlow, UK, 2004.
7 C. Champod, C. J. Lennard, P. Margot and M. Stoilovic, *"Fingerprints and Other Ridge Skin Impressions (International Forensic Science and Investigation)*, CRC Press, Boca Raton, 2004.
8 O. Jensen and E. Nielsen, *Acta Derm.*, 1979, **59**, 139–143.
9 N. Akiba, N. Saitoh and K. Kuroki, *J. Forensic Sci.*, 2007, **55**, 180.
10 M. J. Choi, T. Smoother, A. A. Martin, A. M. McDonagh, P. J. Maynard, C. Lennard and C. Roux, *Forensic Sci. Int.*, 2007, **173**, 154.
11 J. Almog, G. Levinton-Shamuilov, Y. Cohen and M. Azoury, *J. Forensic Sci.*, 2007, **52**, 1057.
12 J. D. James, C. A. Pounds and B. Wilshire, *J. Forensic Sci.*, 1993, **38**, 391.
13 L. K. Seah, U. S. Dinish, W. F. Phang, Z. X. Chao and V. M. Murukeshan, *Forensic Sci. Int.*, 2005, **152**, 249.
14 A. R. W. Jackson and J. M. Jackson, *Forensic Science*, Pearson Prentice House, Harlow, UK, 2004.
15 *Manual of fingerprint development techniques*, ed. V. Bowman, Sandridge, UK, 2nd rev. edn, 2004: Police Scientific Development Branch, Home Office.
16 P. Czekanski, M. Fasola and J. Allison, *J. Forensic Sci.*, 2006, **51**, 1323.
17 M. Colella, A. Parkinson, T. Evans, C. Lennard and C. Roux, *J. Forensic Sci.*, 2009, **54**(3), 583–590.
18 K. K. Bouldin, E. R. Menzel, M. Takatsu and R. H. Murdock, *J. Forensic Sci.*, 2000, **45**, 1239.
19 G. Williams, H. M. McMurray and D. A. Worsley, *J. Forensic Sci.*, 2001, **46**, 1085.
20 G. Williams and N. McMurray, *Forensic Sci. Int.*, 2007, **167**, 102.
21 J. W. Bond, *Rev. Sci. Instrum.*, 2009, **80**, 075108.
22 E. Gutierrez-Redomero, C. Alonso-Rodriguez, L. E. Hernandez-Hurtado and J. L. Rodriguez-Villalba, *Forensic Sci. Int.*, 2011, **208**, 79–90.
23 C. Bersellini, L. Garofano, M. Giannetto, F. Lusardi and G. Mori, *J. Forensic Sci.*, 2001, **46**, 871.
24 G. L. Thomas and T. E. Reynoldson, *J. Phys. D: Appl. Phys.*, 1975, **8**, 724–729.
25 A. L. Beresford and A. R. Hillman, *Anal. Chem.*, 2010, **82**, 483–486.
26 F. Blanchard, B. Carre, F. Bonhomme, P. Biensan, H. Pages and D. Lemordant, *J. Electroanal. Chem.*, 2004, **569**, 203–210.
27 A. Bund and S. Neudeck, *J. Phys. Chem. B*, 2004, **108**, 17845–17850.
28 L. Niu, C. Kvarnstrom and A. Ivaska, *J. Electroanal. Chem.*, 2004, **569**, 151–160.
29 L. Pigani, A. Heras, A. Colina, R. Seeber and J. Lopez-Palacios, *Electrochem. Commun.*, 2004, **6**, 1192–1198.
30 W. Plieth, A. Bund, U. Rammelt, S. Neudeck and L. M. Duc, *Electrochim. Acta*, 2006, **51**, 2366–2372.
31 F. Petraki, S. Kennou, S. Nespurek and M. Biler, *Org. Electron.*, 2010, **11**, 1423–1431.
32 D. C. Martin, J. Wu, C. M. Shaw, Z. King, S. A. Spanninga, S. Richardson-Burns, J. Hendricks and J. Yang, *Polym. Rev.*, 2010, **50**, 340–384.
33 H. K. Song, E. J. Lee and S. M. Oh, *Chem. Mater.*, 2005, **17**, 2232.
34 A. L. Beresford, R. M. Brown, A. R. Hillman and J. W. Bond, *J. Forensic Sci.*, 2012, **57**(1), 93–102.
35 L. B. Groenendall, F. Jonas, D. Freitag, H. Pielartzik and J. R. Reynolds, *Adv. Mater.*, 2000, **12**, 481–494.
36 V. G. Sears, S. M. Bleay, H. L. Bandey and V. J. Bowman, *Sci. Justice*, 2011, DOI: 10.1016/j.scijus.2011.10.006, in press.
37 A. R. Hillman, I. Efimov and K. S. Ryder, *J. Am. Chem. Soc.*, 2005, **127**(47), 16611–16620.
38 A. R. Hillman, S. J. Daisley and S. Bruckenstein, *Phys. Chem. Chem. Phys.*, 2007, **9**, 2379–2388.
39 G. L. Thomas and T. E. Reynoldson, *J. Phys. D: Appl. Phys.*, 1975, **8**, 724.
40 E. G. Tolstopyatova, N. A. Pogulaichenko, S. N. Eliseeva and V. V. Kondratiev, *Russ. J. Electrochem.*, 2009, **45**(3), 252–262.
41 C. Li and T. Imae, *Macromolecules*, 2004, **37**, 2411.
42 Y. Wen, J. Xu, H. He, B. Lu, Y. Li and B. Dong, *J. Electroanal. Chem.*, 2009, **634**, 49–58.
43 G. L. Thomas, *Thin Solid Films*, 1974, **24**, 52.
44 G. L. Thomas, *J. Phys. E: Sci. Instrum.*, 1978, **11**, 722.